

Original Article

# A Low-Cost Particulate Matter Sensor System Using Optical Sensors for Efficient Air Pollution Monitoring

Kalali Das<sup>1</sup>, Sagnik Ghosh<sup>2</sup>, Himadri Sekhar Dutta<sup>3</sup>

<sup>1,3</sup>Department of Electronics and Communication Engineering, Kalyani Government Engineering College, West Bengal, India.

<sup>2</sup>Department of Computer Science and Engineering, IIT Kharagpur, West Bengal, India.

<sup>1</sup>Corresponding Author : [d.kakali.05@gmail.com](mailto:d.kakali.05@gmail.com)

Received: 02 October 2024

Revised: 02 November 2024

Accepted: 01 December 2024

Published: 31 December 2024

**Abstract** - Air pollution is a significant societal concern as it can have profound health implications, leading to illnesses and even fatalities among individuals. Particulate Matter (PM), a common form of air pollution, is known to be particularly harmful, contributing to heart and respiratory issues. This research addresses the issue of air pollution, specifically the health risks associated with Particulate Matter (PM<sub>2.5</sub>). The study aims to establish baseline PM<sub>2.5</sub> concentration levels, an essential step toward enhancing air quality standards, particularly in developing countries. This study introduces a novel and economical detection approach that leverages readily accessible sensors backed by comprehensive data gathered from diverse settings in West Bengal. The system aims to precisely assess PM levels in different conditions using digital signal processing methods to reduce noise and maintain reliable calibration. This research highlights the commitment to addressing air pollution and demonstrates the approach's effectiveness through detailed experimental analysis. This work can significantly contribute to creating safer, healthier environments globally.

**Keywords** - Air pollution, Optical PM sensors, Low-cost PM sensor system, Digital signal processing, Air quality.

## 1. Introduction

Improving quality of life has led to a growing focus on air quality in the twenty-first century. Numerous studies have shown that indoor air can be more harmful than outdoor air [1]. In most developing countries, 90% of rural households and approximately half of the world's population rely on unprocessed biomass for open fires and inefficient cooking stoves indoors. These ineffective cooking methods contribute to Indoor Air Pollution (IAP). They can hurt the health of women and young children frequently exposed to this polluted environment [2]. Burning biomass and coal emits a range of dangerous pollutants, including Particulate Matter (PM), Nitrogen Dioxide (NO<sub>2</sub>), Carbon Monoxide (CO), Sulphur Oxides, polycyclic organic matter, and formaldehyde.

The poor Indoor-Air-Quality (I-A-Q) condition has been identified as the ninth-biggest global disease burden risk [3]. The WHO indicated that in 2012, over four million three hundred thousand early deaths were associated with air pollution inside buildings, compared to three million seven hundred thousand fatalities caused by environmental air contamination [4]. The Health Metrics and Evaluation Institute attributed 2.57 million early deaths to indoor air pollution in 2016. Asia, Africa, America, and Europe were responsible for 74%, 23%, 2% and 1% of these deaths,

respectively [5]. Particulate Matter (PM) is a crucial indicator of Indoor Air Quality (IAQ), measuring all the solid and liquid particles in the air. Particulate Matter (PM) is closely associated with numerous severe health complications. Being exposed to PM can result in critical conditions like heart attacks, strokes, and heart failure [6]. It also affects respiratory problems, including asthma and Chronic-Obstructive-Pulmonary-Disease (COPD).

Additionally, research has revealed that tiny particles measuring less than 200 nanometers can penetrate deep into the brain, raising concerns about their potential role in neurodegenerative diseases like Alzheimer's disease. This alarming capability of particulate matter to invade vital organs underscores the urgent need to address air quality and its impact on public health [7, 8]. According to a 2014 report from the WHO, 4.3 million individuals and 3.7 million individuals die due to inadequate indoor and outdoor air pollution, respectively [4, 9].

Air pollution from Particulate Matter (PM), including golden dust and tiny particles, is deteriorating each year in numerous countries in Asia, Africa, the Middle East, and Europe. This type of pollution originates from factors such as automobiles, coal combustion, and cooking indoors. As the



quality of life improves, so does the understanding of particulate air pollution, which drives the creation of technologies such as air purifiers and monitoring systems. Nevertheless, a majority of these systems depend on low-cost sensors, leading to a reduction in accuracy and effectiveness. [10-12].

Low-cost sensors are known for their compact size and their capability to link up with microcontrollers to build small, adaptable measurement tools. Their high level of portability and minimal energy usage are also distinguishing features. They can be utilized in diverse scenarios, establish measurement networks using various concepts, and serve a multitude of other functions.

Atmospheric PM is typically assessed using two primary criteria: particle mass concentration, which indicates the mass of a particle within a specific volume (usually measured in  $\mu\text{g}/\text{m}^3$ ), and particle number concentration, which represents the quantity of particles within a specific volume (measured in particles/ $\text{m}^3$ ). Even so, additional metrics offer vital insights into the characteristics of airborne particulate matter. Another important aspect of PM is the Particle Size Distribution (PSD), which denotes the particle concentration (either mass or number) measured across various particle sizes.

A range of techniques have been proposed for measuring particulates, such as the gravimetric method, a technique for measurement that relies on beta radiation, a resonance-frequency measurement technique, and a method utilizing light scattering. [13-21]. The gravimetric method [22] is accepted as a standard approach due to its high precision; however, it tends to be costly and extensive, rendering it impractical for I-o-T devices or household appliances. The Beta-ray Absorption Method (BAM) [23] involves:

- The collection of particulates on filter paper.
- The emission of beta-rays.
- The measurement of concentration is based on the difference between the absorbed and transmitted beta-rays.

Although this method offers lower accuracy than the gravimetric technique, it is generally more affordable and compact. Tapered Element Oscillates Microbalance (TEOM) [24] and detects changes in resonance frequency to measure particulate concentration. Finally, the light scattering method assesses particle concentration by examining the intensity of scattered light when exposed to a laser or infrared LED. Inexpensive light-scattering methods are mainly used in IoT devices or air purification systems. External factors like temperature and humidity greatly affect the light scattering technique and may lack accuracy and stability when responding to particle sizes and shapes [25]. Research studies have also been carried out on assessing particulate matter in

outdoor settings [26-28]. This investigation seeks to create a precise and cost-efficient system for monitoring outdoor air quality by utilizing various low-cost sensors to obtain accurate data from less accurate sensors. The monitoring system for PM sensors is established using an optical sensing and scattering approach.

The PM detection and monitoring system has been evaluated in various outdoor environments to measure PM 2.5 levels in micrograms per cubic meter. This evaluation includes high-traffic roads in Kolkata, West Bengal, India, and Bankura, which are located in the western region of West Bengal. The system was also tested in the renowned industrial city of Kharagpur, situated in the West-Medinipur District in West Bengal, and in Darjeeling, the highest-altitude town in the northern region of West Bengal, located in the Eastern Himalayas with an average elevation of 6,709 feet. The collected data has been used to calculate the average PM2.5 values in  $\mu\text{g}/\text{m}^3$ . In-depth graphical analyses have been conducted to evaluate the performance of the PM2.5 sensor monitoring system.

The document is organized into distinct sections: Section 2 provides a summary of relevant literature, while Section 3 examines a sensor-driven system designed for detecting particulate matter in outdoor environments. Section 4 outlines the method for precisely measuring PM2.5. Section 5 assesses the system's performance, highlighting its reliability and precision through visual representation. Finally, Section 6 will summarize the content and propose avenues for future research.

## 2. Related Works

Several studies have explored the application of calibrations for inexpensive sensors. Zaidan et al. [28] suggested a virtual sensor system utilizing machine learning. This approach involves gathering precise air quality data (such as PM2.5 and CO<sub>2</sub>) from a reliable instrument and utilizing artificial intelligence to forecast air quality based on low-cost sensors in real-world settings.

Due to the use of machine learning to rectify differences between the reference instrument and low-cost sensors, their system can produce more precise results. They also demonstrated an enhancement in the accuracy of the low-cost sensor while compensating for differences with the reference instrument. An analogy was drawn between the estimated mean daily concentration levels and the reference measurements and the hourly structure of outcomes delivered at each station to evaluate the effectiveness of data integration.

Accurate data collection necessitates gathering significant data from the reference instrument and sensors. Challenges in on-site measurement and learning present a limitation to their system. Alfano et al. [13] conducted a study

on the measurement of acceptable dust. The study focused on techniques for categorizing and measuring dust particles by their size.

The authors explained the core concepts of the gravimetric technique, tapered element oscillating microbalance, attenuation of beta radiation, optical-particle counters, and scattering of light (particularly Mie theory) as methods for measuring particulate matter. They also described various laboratory chamber setups capable of accurately measuring particulate matter. They underscored the importance of adjusting for temperature and humidity to improve the precision of optical sensors. Their study is valuable because it emphasizes the accuracy of various PM sensors available in the market.

S. K. Sharma et al. conducted an analysis of the elemental makeup of fine Particulate Matter (PM<sub>2.5</sub>) in Delhi, India, spanning from January 2017 to December 2021 [29]. Their findings revealed that during the post-monsoon season, sulphur, chlorine, potassium, calcium, and iron were in the highest concentrations. Additionally, the elemental composition of PM<sub>2.5</sub> accounted for 10% of the total PM<sub>2.5</sub> over the five years. Principal Component Analysis (PCA) identified the five main sources [crustal/soil/road dust, combustion (BB+FFC), Vehicular Emissions (VE), Industrial Emissions (IE) and mixed source (Ti, Cr and Mo rich-source)] of PM<sub>2.5</sub> in Delhi, India.

Miskell et al. [30] introduced straightforward, remote, and ongoing calibration methods for hierarchical networks involving deploying high-precision instruments (proxies) alongside numerous affordable sensors. To estimate the slope and offset, the average and standard deviation of the sensor readings are aligned with the values obtained from a proxy during the same timeframe. Rogulski et al. conducted a prolonged assessment of low-cost PM<sub>10</sub> measurements and compared them to the findings of the reference air quality monitoring station under various atmospheric conditions. These included cold days (with a minimum temperature below  $-10^{\circ}\text{C}$ ) with high relative humidity reaching 95%, and days with a maximum temperature above  $30^{\circ}\text{C}$  and low relative humidity at around 25%. They determined the correlation coefficients for both devices with the reference station, resulting in values of  $r = 0.91$  and  $r = 0.94$ , respectively.

The long-term percentage errors were minimized to a maximum of about 20%, with average percentage errors typically staying around 10% [31]. In their study, Cho et al. introduced a practical system for particulate matter sensing and accurate calibration utilizing low-cost commercial sensors, allowing noisy and imprecise PM sensors to measure ambient air pollution. The paper explores three types of errors related to the light scattering technique: short-term noise, variability between different parts, and influences from temperature and humidity [32]. The research conducted by

Motlagh et al. [33] aimed to create a system that employed affordable wearable sensors to precisely gauge the daily exposure of public transport riders to pollutants. The level of exposure was evaluated by monitoring particulate matter. Nevertheless, the study focused solely on the differences between commercial sensors and did not provide details on sensor calibration or possible error factors.

Conversely, Gressent et al. [34] carried out an extensive project aimed at tracking air pollution across the city. Due to the sparse and expensive nature of the reference station network, the researchers installed numerous low-cost sensors on buildings. Others were placed onto moving vehicles to assess the level of particulate matter in the downtown area. The data collected from these sensors was used to map air quality at an urban scale, emphasizing the potential advantages of these insights in creating dispersion models.

Clements et al. [35] described their participation in a two-day workshop where they examined the following topics:

- Practical techniques for implementing and refining cost-effective sensor systems
- Initiatives focused on data standardization and the creation of databases
- Progress in sensor calibration, data structuring, data analysis, and visualization
- A dialogue within the community

The discussion with community members highlighted improvements in knowledge and project outcomes while emphasizing significant questions, unresolved issues, and technical challenges related to inexpensive air quality monitors.

To further assess how well low-cost air sensors measure the effects of different indoor factors and indoor PM<sub>2.5</sub> levels, Bi et al. estimated infiltration factors (Finf). These factors represent the fraction of outdoor PM<sub>2.5</sub> that enters indoor spaces and contributes to indoor PM<sub>2.5</sub> levels, and they were compared to existing research. To calculate Finf, they utilized data from times when there were no indoor sources (e.g., during the middle of the night, from 11 pm to 5 am) [36].

Mendez et al. conducted a research study to assess the levels of PM<sub>2.5</sub> pollution in four cities along the U.S.–Mexico border. These urban areas include Brownsville, Edinburg, Weslaco, and Port Isabel, located in the Lower Rio Grande Valley Region of South Texas. The investigation occurred from March 1, 2021, to March 31, 2022, involving Mendez et al. carrying out a research study to evaluate the levels of PM<sub>2.5</sub> pollution in four cities along the U.S.–Mexico border. These metropolitan areas comprise Brownsville, Edinburg, Weslaco, and Port Isabel, situated in the Lower Rio Grande Valley Region of South Texas. The study took place from March 1, 2021, through March 31, 2022, and included a year-

long sampling initiative. TSI BlueSky™ Air Quality Monitors were simultaneously deployed at 11 locations within these cities. The PM2.5 levels recorded by these monitors over 24 hours were subsequently compared with the ambient PM2.5 data collected from the Texas Commission on Environmental Quality (TCEQ) Continuous Ambient Monitoring Station (CAMS) sites. This comparison aimed to identify the spatial and temporal variations in pollutant levels at the local level. The results indicated limited to moderate variations in PM2.5 concentrations throughout the area. The findings implied that low-cost sensors alongside CAMS locations could enhance community monitoring efforts and deliver real-time insights into the spatiotemporal patterns of PM2.5 pollution [37].

### 3. System for Sensing and Calibrating Particulate Matter

Figure 1 includes a block diagram along with the visual representation of the PM sensing system. Table 1 displays the components utilized in the system.

#### 3.1. Laser Diode Principle

The highly directed nature of a laser diode beam, also known as its high directionality or low divergence, can be explained using the principles of wave optics and the properties of stimulated emission in a laser, as shown in Figure 2. In a laser diode, electrons in a semiconductor material are excited to a higher energy state. When they return to a lower energy state, they emit photons. If an existing photon triggers this process, the emitted photon will possess an identical phase, direction, and frequency as the photon that stimulated it. Consequently, the emitted light is highly coherent, indicating that the waves are in sync and maintain a consistent relationship between each photon's phase. This coherence leads to constructive interference, which produces a well-defined and highly directed beam of light.

Table 1. Name of different components with description

Sl. No.	Name	Description
1	Laser	650nm
2	Photodetector	3.3V-5V
3	Humidity Sensor	DHT-11
4	Pressure Sensor	BMP-180
5	Temperature Sensor	LM35
6	Node MCU	ESP-01/3.3V
7	Resistances	100ohm

The laser diode contains an optical cavity or resonator created by two parallel polished surfaces. The resonator is set up between the laser diode and the photodetector. This cavity ensures that only the light traveling parallel to the cavity's axis is amplified through multiple reflections. Other directions are not effectively amplified and do not contribute to the output beam. The resonator's design ensures that the output beam is highly collimated (parallel), resulting in a low-divergence, highly directional beam. The directionality of the laser beam can be quantitatively described by considering the diffraction of light. According to the diffraction limit, a laser beam's divergence angle ( $\theta$ ) is inversely related to the size of the emitting aperture (or the width of the active region in the laser diode).

$$\theta = \frac{\lambda}{w} \tag{1}$$

Where,  $\lambda$  is the wavelength of the laser light, and  $w$  is the width of the emitting region (aperture).

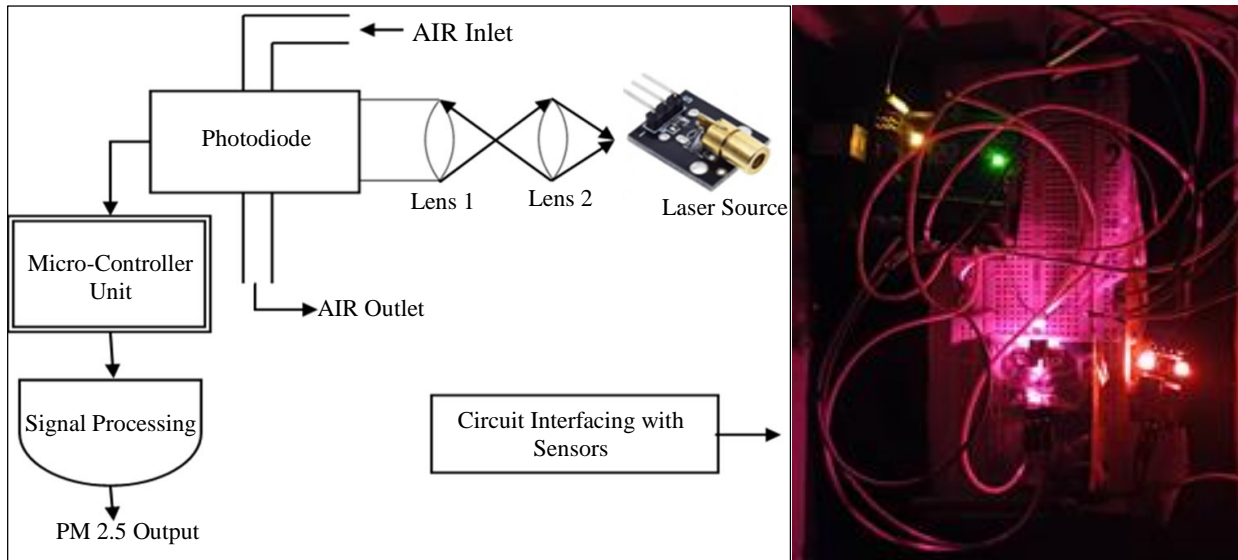
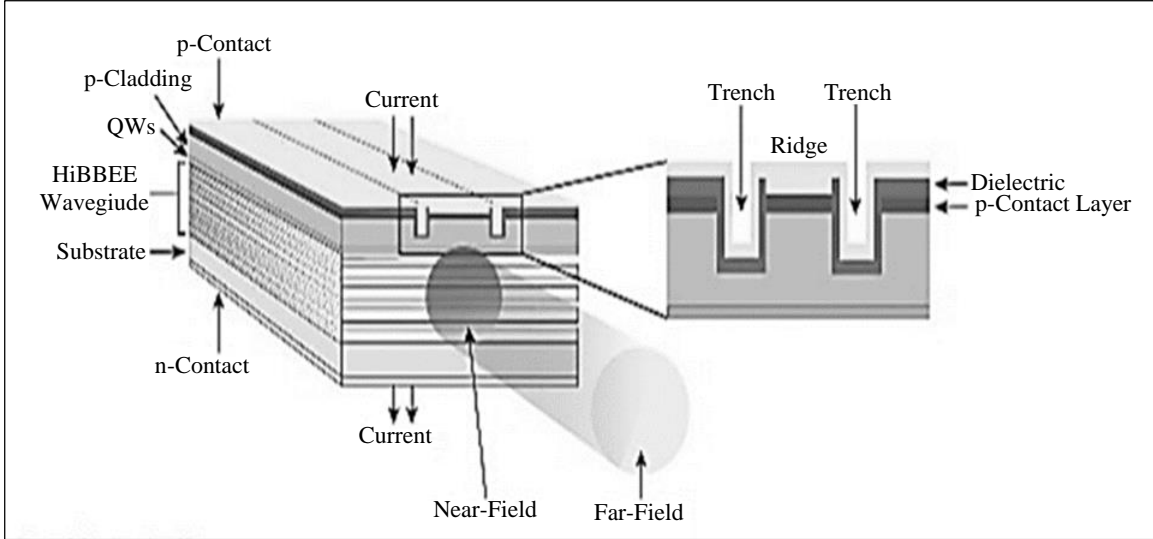
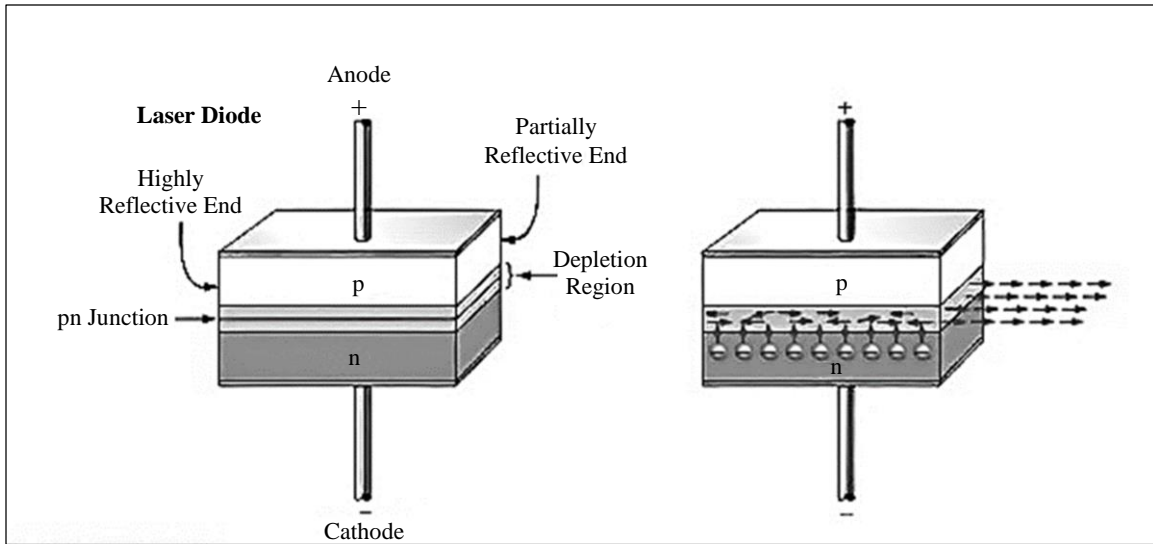


Fig. 1 Block diagram along with the visual representation of the PM sensing system



(a)



(b)

Fig. 2 Laser diode: (a) schematic diagram, and (b) Working principle.

The emitting region of a laser diode is small, resulting in a small  $w$ . The optical resonator's coherence and design help maintain minimal beam divergence. The output beam of a laser diode typically resembles a Gaussian beam, defined by its waist size ( $w_0$ ) and Rayleigh range ( $z_r$ ). The beam divergence ( $\theta$ ) for a Gaussian beam can be expressed as:

$$\theta \approx \frac{\lambda}{\pi w_0} \quad (2)$$

Where  $\theta$  is the half-angle divergence of the beam and  $w_0$  is the waist radius of the beam (the narrowest part of the beam).

The focused nature of a laser beam, particularly its Gaussian shape, can be understood by applying the principles

of Gaussian beam optics and diffraction theory. Frequently, a laser beam exhibits a Gaussian intensity pattern, indicating that the distribution of the beam's electric field on a plane perpendicular to its direction of movement has a Gaussian shape. The magnitude of the electric field  $E(r, z)$  of a Gaussian beam at a distance  $z$  from the beam waist can be mathematically represented as:

$$E(r, z) = E_0 \frac{w_0}{w(z)} \exp\left(-\frac{r^2}{w(z)^2}\right) \exp\left(-i\left(kz + \frac{kr^2}{R(z)} - \psi(z)\right)\right) \quad (3)$$

Where:

$r$  is the radial distance from the beam axis.

$z$  is the distance along the propagation direction.

$E_0$  is the electric field amplitude at the beam waist.

$w_0$  is the waist radius (the smallest radius of the beam).

$w(z)$  is the beam radius at a distance  $z$ , defined as:

$$w(z) = w_0 \sqrt{1 + \left(\frac{z}{z_R}\right)^2} \quad (4)$$

$k$  is the wavenumber,  $k=2\pi/\lambda$

$R(z)$  is the radius of curvature of the beam's wavefronts, defined as:

$$R(z) = z \left(1 + \left(\frac{z_R}{z}\right)^2\right) \quad (5)$$

$\psi(z)$  is the Gouy phase shift, defined as:

$$\psi(z) = \text{atan}\left(\frac{z}{z_R}\right) \quad (6)$$

$z_R$  is the Rayleigh range, given by:

$$z_R = \frac{\pi w_0^2}{\lambda} \quad (7)$$

Laser scattering happens when a laser beam interacts with particles, molecules, or irregularities in a medium, causing the beam's light to change direction from its original path. The scattering can reveal the particles' size, shape, and composition, causing the scattering.

Rayleigh, Mie, and Raman are the three primary types of scattering, each governed by distinct physical principles and equations. Mie scattering occurs when the particles causing the scattering are similar in size to the wavelength of the incident light. This scattering is more intricate than Rayleigh and applies to larger particles such as dust, water droplets, and other aerosols.

### 3.2. Mie Scattering Coefficient

Mie scattering is described by a series of complex equations derived from Maxwell's equations, taking into account the size parameter  $x$ , which is defined as:

$$x = \frac{2\pi r'}{\lambda} \quad (8)$$

Where:

$r'$  is the radius of the scattering particle.

$\lambda$  is the wavelength of the incident light.

The Mie scattering coefficients  $a_n$  and  $b_n$  are obtained by solving Maxwell's equations, and the scattering efficiency  $Q_{sc}$  is given by:

$$Q_{sc} = \frac{2}{x^2} \sum_{n=1}^{\infty} (2n+1) (|a_n|^2 + |b_n|^2) \quad (9)$$

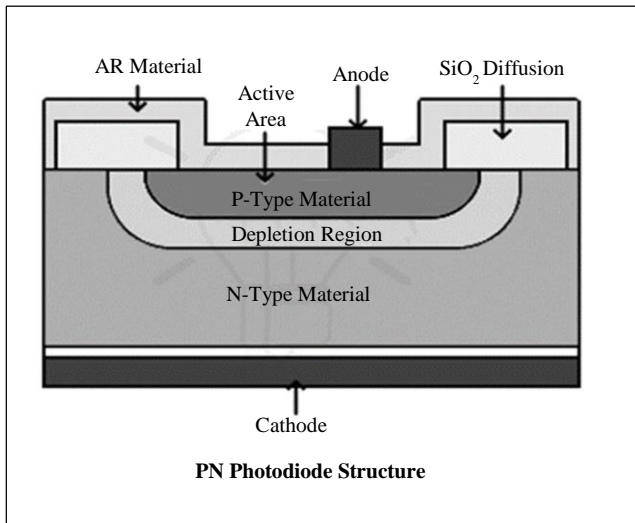
Where,  $n$  is the mode number, and  $a_n$  and  $b_n$  are the Mie coefficients, which depend on the size parameter  $x$  and the refractive index of the particle relative to the surrounding medium. The intensity distribution of scattered light depends on the size parameter  $x$  and the angle  $\theta$ .

### 3.3. Photodiode Principle

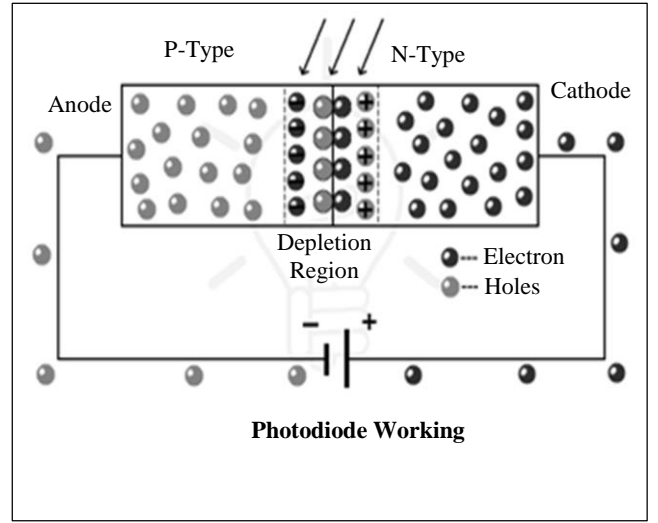
A photodiode turns light into electric current using semiconducting material. It works by the photoelectric effect, which produces electron-hole pairs when photons hit the material, causing electric current flow under applied voltage.

#### 3.3.1. Photodiode Structure and Operation

Figure 3(a) shows the basic structure of a photodiode where the p-type and n-type regions with the depletion region are in between, and Figure 3(b) defines its operation under light exposure.



(a)



(b)

Fig. 3 (a) Photodiode structure, and (b) Current flow in photodiode.

A photodiode, constructed from semiconductors such as silicon featuring a p-n junction, comprises P-type and N-type regions and a depletion region. The photodiode functions in photoconductive mode. Upon connection to an external circuit, the movement of these charge carriers gives rise to a photocurrent. In the case of a reverse-biased PN junction diode, the depletion region expands, leading to reduced capacitance, improved response speed, and the generation of reverse current. When a photon or light ray possessing energy more significant than the energy gap impacts the photodiode, it displaces an electron from it, forming an electron-hole pair. The resulting flow of electric charge, referred to as photocurrent, increases in direct proportion to the strength of the incoming light.

In photodiodes, a current flow remains even in the absence of light sources or photons striking its junction. This current is referred to as dark current and is quite small, typically in the microampere range. It is similar to the leakage current observed in a standard PN junction diode. The unwanted current under reverse bias is directly proportional to temperature and needs to be minimized to enhance the sensitivity of the photodiode. The overall current of any photodiode is the combination of the photocurrent and the dark current, is directly proportional to temperature and needs to be minimized to enhance the sensitivity of the photodiode. The overall current of any photodiode is the combination of the photocurrent and the dark current. The photocurrent ( $I_p$ ) generated in the photodiode is proportional to the incident light power and can be expressed as:

$$I_p = \eta \frac{P_{op}}{h\nu} q \quad (10)$$

Where:

- $\eta$  is the quantum efficiency of the photodiode.
- $P_{op}$  is the optical power of the incident light.
- $h$  is Planck's constant.
- $\nu$  is the frequency of the incident light.
- $q$  is the charge of an electron.

In reverse bias, the total current  $I$  through the photodiode is the sum of the dark current  $I_d$  and the photocurrent  $I_p$ . The I-V characteristic equation of a photodiode in the reverse bias region is given by:

$$I = I_d - I_p \quad (11)$$

$$I = I_s \left( e^{\frac{qV}{kT}} - 1 \right) - I_p \quad (12)$$

Where:

- $I_s$  is the saturation current.
- $V$  is the applied reverse bias voltage.
- $k$  is Boltzmann's constant.
- $T$  is the absolute temperature.

The conversion efficiency of incident light into an electrical signal in a photodiode is determined by its responsivity, represented as  $R$ . Responsivity is commonly expressed in A/W (amperes per watt).

$$R = \frac{I_p}{P_{op}} = \eta \frac{q}{h\nu} \quad (13)$$

When calculating the output voltage of a photodiode based on the scattering of PM 2.5 particles, a common approach includes using a configuration where the photodiode detects the intensity of scattered light from a laser beam interacting with the particles in the air.

### 3.3.2. Scattering of Light by PM 2.5 Particles

The light scattering of a laser beam passing through air with PM 2.5 particles occurs in different directions. The amount of scattered light is determined by the size and concentration of the particles, and Mie scattering principles govern this process since PM 2.5 particles are approximately the same size as the wavelength of visible light.

### 3.3.3. Photodiode Detection

A photodiode is positioned at a specific angle (typically  $90^\circ$  or  $45^\circ$  to the laser beam) to detect the scattered light. The intensity of the scattered light hitting the photodiode is converted into an electrical current proportional to the light intensity.

### 3.3.4. Photocurrent Generation

The photodiode generates a photocurrent ( $I_p$ ) proportional to the intensity of the scattered light, related to the concentration of PM 2.5 particles in the air.

### 3.3.5. Conversion to Output Voltage

The photocurrent generated by the photodiode is typically converted to a voltage using a transimpedance amplifier (TIA). The output voltage  $V_o$  of the photodiode circuit can be expressed as:

$$V_o = I_p R_f \quad (14)$$

Where:  $R_f$  is the feedback resistor in the transimpedance amplifier.

The current produced by the photodiode ( $I_p$ ) increases in direct proportion to light intensity. The photodiode detects scattered light ( $I_{sct}$ ) in proportion to the concentration of PM2.5 particles ( $C_{PM2.5}$ ):  $I_p \propto I_{sct} \propto C_{PM2.5}$ . Thus, the output voltage is proportional to the PM 2.5 concentration:

$$V_o = k C_{PM2.5} \quad (15)$$

Where  $k$  is a proportionality constant that depends on factors such as the sensitivity of the photodiode, the scattering angle, the laser power, and the transimpedance amplifier gain.

To establish the relationship between  $V_o$  and CPM2.5, various graphical analyses were conducted on the concentrations of PM 2.5 particles. This approach can be widely used in commercial particle sensors for air quality monitoring, where the output voltage is interpreted to give the concentration of particulate matter like PM 2.5.

#### 4. Operation Principle of the PM2.5 Optical Sensor Monitoring System

The PM2.5 optical sensor monitoring system's source module is equipped with a laser diode that emits light at a wavelength of 650nm (red light) and operates on a 5V power supply. When a laser diode emits light, it generally spreads out as a divergent beam. This light would disperse if not collimated, losing its focus and intensity while traveling.

The essential part of a collimator is the collimating lens, which is positioned in front of the laser diode. This lens, typically a convex lens (or a combination of lenses), is designed with a focal length that matches the characteristics of the laser beam. The positioning of the lens relative to the laser diode is crucial. The laser diode output must align with the focal point of the lens. As the divergent laser light travels through the lens, the light rays are refracted, causing them to align and become parallel.

Once the divergent light rays pass through the collimating lens, they emerge as a parallel or nearly parallel beam. The precision of the lens and the alignment determine the quality of collimation, which refers to how parallel the beam is. A collimated laser beam maintains its diameter and intensity over a longer distance than a non-collimated beam. This alignment of parallel and highly focused beams is crucial as the laser needs to interact with particles at a specific distance from the source. As a result, the beam of rays is perfectly coherent and collimated. The emitted laser beam is aimed into the air chamber that contains the air sample.

When tiny particles (PM2.5 or smaller) encounter the laser beam, they disperse in various directions. The sensor's photodetector is strategically placed to detect the dispersed light. The location of the photodetector is determined by the sensor's setup and the specific characteristics of the particles it intends to detect. The photodetector's surface reacts to the intensity and pattern of the incoming light.

The electrical signal produced by the photodetector when it is hit by scattered light is directly related to the light's intensity. The size and concentration of the particles determine the intensity and pattern of the scattered light. As particles increase, so does the amount of light scattered. The PM 2.5 sensor uses a laser diode to emit a focused light beam into an air sampling chamber.

When light travels through the air, it comes across particles such as dust, pollen, or smoke (PM2.5 or smaller).

These particles cause the light to scatter in different directions. PM2.5 sensors often utilize photodiodes due to their quick response time, sensitivity, and ability to work with low light levels. An electrical signal is produced when the photodetector converts the optical (scattered light) signal. This is typically accomplished using materials demonstrating the photoelectric effect, where incoming photons create electron-hole pairs, resulting in a measurable current or voltage.

The PM2.5 sensors, because of their sensitivity, rapid response time, and ability to function in low light conditions. The sensor's internal electronics are then evaluated, and the electric signal produced by the photodetector is examined. This evaluation involves boosting the signal and reducing noise, and the analog signals are converted into digital patterns. The magnitude of the signal corresponds to the quantity of particles in the air. A higher number of particles results in greater light scattering, which generates a stronger signal from the photodetector.

In PM2.5 sensors, the photodetector detects the scattered light produced by particulate matter in the air, converts it into an electrical signal, and then analyzes it to determine the particle concentration. The accuracy of air quality measurements from the sensor, particularly for small particles like PM2.5, depends greatly on the precision and sensitivity of the photodetector.

The proposed design features a difference in diameter between the inlet and outlet tubes for air, which serves a specific purpose in air sampling and particle identification. A reduced diameter for the air inlet tube plays a critical role in controlling the airflow into the sensor's detection chamber. This restriction ensures that the chamber receives air at a controlled, slower pace, vital for accurate measurement. Slower airflow allows for increased interaction between particles and the laser beam, improving detection capabilities.

A wider outlet tube facilitates the smoother air exit from the chamber, maintaining a consistent flow of air through the sensor and continuously replacing the sampled air with fresh air. The larger diameter also reduces resistance, allowing air to exit the chamber smoothly without affecting the air entering the chamber. The reduced airflow speed resulting from the smaller inlet tube allows particles to remain in the detection chamber for longer, increasing the chances of particles crossing the path of the laser beam and resulting in more detectable scattering events for the photodetector. This is especially important for detecting smaller particles like PM2.5, which present a greater challenge for detection.

The particulate matter monitoring sensor system was utilized to measure the concentration of particulate matter. Figure 1(a) shows how the PM monitoring system works. It relies on tightly focused light transmission with minimal diffusion. A red 650 nm Laser source emits a highly directed,



intense light beam into a measurement chamber. When dust is present, the light scatters off the particles and the scattered light is detected by the internal photodetector (photodiode). Submicron dust particles near 1 μm are nearly spherical, causing the scattering light to have the most significant value, especially at low angles. The test chamber's inlet and outlet tubes are positioned through optical windows to allow accurate data collection. The lower part of the inlet tube contains a smaller nozzle with an inner diameter of 2 mm.

In comparison, the outlet has an extended inner diameter of about 8 mm and an overall diameter of 12 mm. Both tubes are vertically secured with ring clamps on a support stand fixed on the chamber, and their central axis is carefully adjusted to be at a right angle with the laser beam. The laser beam is 7 mm away from the lower end of the inlet tube and 8 mm away from the upper end of the outlet tube. The inlet tube's reduced nozzle and the larger diameter of the outlet tube are designed to minimize diffusion loss. The outlet tube's flow rate is four times that of the inlet.

The PM concentration was recorded at various volumes and under multiple scenarios across different geographical locations in West Bengal. The sensing system generated output in the form of voltage values, which were then used to determine the concentration of particles through signal processing techniques. The Butterworth digital filter is recognized for its consistent frequency response. It has no variations in the passband or the stopband, effectively reducing high-frequency noise while maintaining a seamless shift from passband to stopband.

Due to its consistent frequency response in the passband, it maintains the magnitude of the signal's low-frequency components. While not a linear-phase filter, the Butterworth filter introduces relatively minimal phase distortion compared to other filter types. The filter aids in diminishing noise and creating smoother, more understandable data. Therefore, using a low-pass Butterworth digital filter to standardize data can strike a balance between reducing noise and preserving the signal, ensuring that the data remains valuable and accurate for further analysis or processing.

The detected output signal is processed using a low-pass Butterworth digital filter, followed by a moving average block to obtain a smoothed signal suitable for further processing. This smoothed data is then used to calibrate and estimate

PM2.5 values. The data is again passed through the above stages for re-estimation and better results. A block diagram for the signal processing pipeline is shown in Figure 4.

The moving average is a robust and versatile smoothing technique that balances noise reduction, computational efficiency, and ease of implementation. While more sophisticated methods are available, the moving average remains a popular choice due to its straightforward approach and reliable performance in a wide range of scenarios. The moving average is often the preferred method for applications where simplicity and real-time performance are critical.

Calibrating voltage values to PM2.5 concentration involves fitting a polynomial equation (in this case, a quadratic equation) based on known reference data points. The general form of a quadratic calibration equation is:

$$PM2.5 = a.V^2 + b.V + C,$$

Where V is the voltage, and a, b, and c are the coefficients to be determined. It seems that three conditions were taken into account during the calculation of the coefficients for the quadratic model.

The first set of values represents the hot and humid conditions during the months of April, May, and June. The second set of values indicates the monsoon conditions in the months of July and August. The last set of readings is taken for the winter months of November and December. The yearly averages of the data have been depicted, utilizing three separate curve fitting values, which were averaged for calibration purposes.

*Step-by-Step Calibration Process*

1. Collect Reference Data: It is understood that a definitive set of voltage values exists alongside their corresponding PM2.5 concentrations. This data is typically sourced from a reliable reference.
2. Fit a Quadratic Model: It was noted that a quadratic model was fitted using the reference data.
3. Apply the Model: The fitted quadratic model converted the voltage readings into PM2.5 values.

A set of values for a, b, and c has been obtained. The average values are utilized for subsequent processing. Table 2 presents the obtained values.

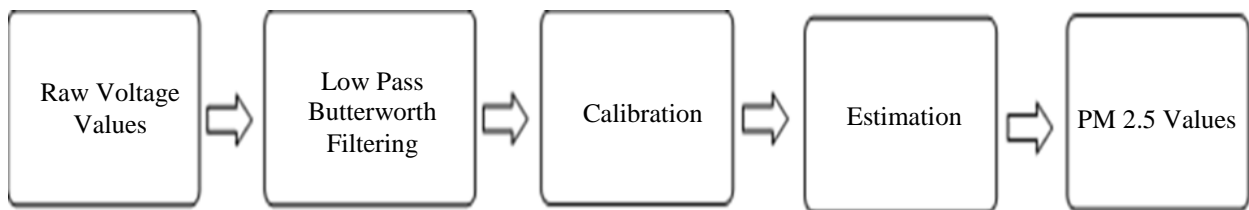


Fig. 4 A block diagram for the signal processing pipeline

**Table 2. Set of values for a, b, c**

SL. No.	Values Obtained
1	a = 1.4026827100679333, b = 0.999031344146858, c = 0.9673428813078239
2	a = - 7.990988084571653, b = 6.552790467657304, c = - 13.148583188293428
3	a = - 4.676957884225419, b = 35.674031191617665, c = - 32.18827001994484

Kalman filtering is a sophisticated estimation technique that outperforms simpler methods like moving averages when it comes to systems with known dynamics and noisy measurements. Its ability to optimally integrate predictions and new data makes it a cornerstone in fields ranging from robotics to finance. When accurate real-time estimation is critical, and the system model and noise characteristics are well understood, Kalman filtering is often the method of choice. Kalman filtering operates by iteratively updating estimates of the system's state using a two-step process:

- Prediction Step: The filter uses the current state estimate and a mathematical model of the system's dynamics to predict the next state.
- Update Step: The predicted state is then updated using the new measurement, considering both the predicted uncertainty and the measurement uncertainty.

This combination of prediction and correction allows Kalman filtering to provide more accurate estimates than simply relying on raw measurements. The parameters of the

Kalman filter, such as the initial state and covariance, transition matrices, and observation matrices, are adjusted based on the data characteristics.

### 5. Results and Discussion

Figure 5(a) suggests that the PM2.5 concentrations are less sensitive to changes in volume at higher temperatures, maintaining near-constant values. However, at moderate temperatures (T2), the PM2.5 concentration increases more noticeably with volume. This could imply that, at certain temperature ranges, the air's capacity to hold particulate matter varies, possibly due to changes in air density or the chemical properties of the particulates at different temperatures. The humidity (71%) and pressure (99437.44 Pa) remain constant, indicating that these factors are not influencing the variations observed.

Figure 5(b) shows the yearly average PM2.5 levels across four cities in West Bengal: Darjeeling, Bankura, Kharagpur, and Kolkata. The data reveals a stark contrast in air quality across these cities. The substantial variation in PM2.5 levels among these cities suggests differences in urbanization, industrial activities, and local environmental policies.

Kolkata, being a major urban center with high traffic density and industrial activity, exhibits the highest pollution levels, which raises public health concerns. Kharagpur, also an industrial town, displays elevated levels but to a lesser extent. In contrast, with its higher elevation and possibly stricter pollution control due to its tourist appeal, Darjeeling demonstrates the lowest PM2.5 levels, indicating better air quality. These findings underscore the need for targeted air quality management strategies in highly polluted cities like Kolkata and Kharagpur.

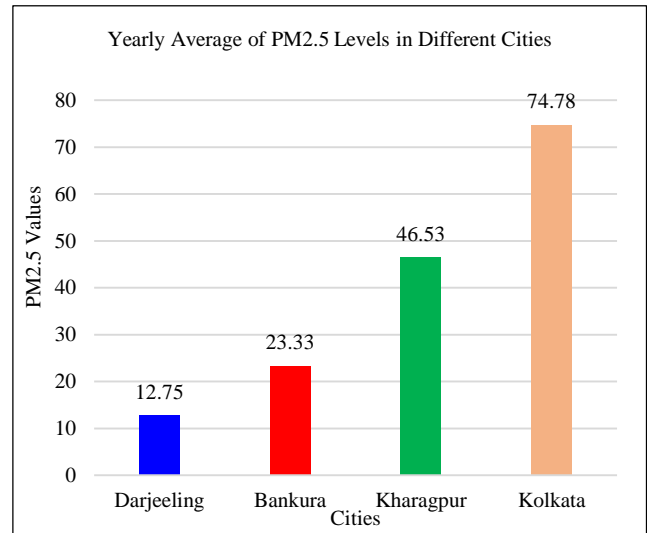
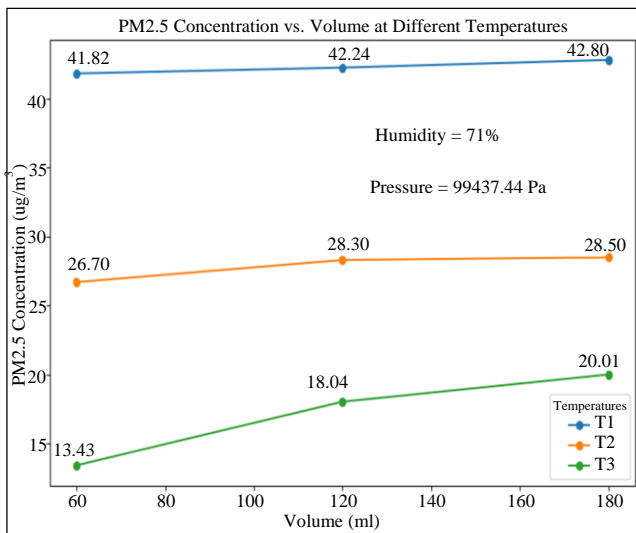


**Fig. 5(a) PM2.5 concentration v/s Volume at different temperatures, and (b) Yearly average of PM2.5 levels in different cities of West Bengal.**

Figure 6(a) provides a comparative analysis of the yearly average PM2.5 levels across various cities in West Bengal under different humidity conditions. The cities considered are Manebhanjan, Darjeeling, Puri, Purulia, and Kolkata. The key observations are stated below:

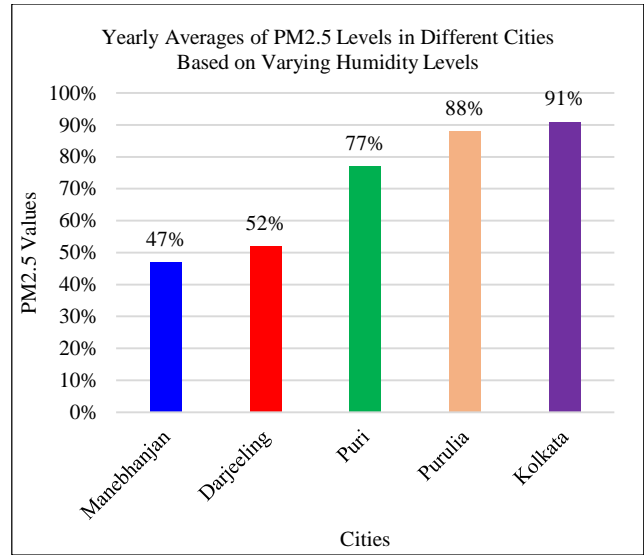
- **Humidity's Impact on PM2.5 Levels:** The graph illustrates that PM2.5 levels vary significantly with changes in humidity. Higher humidity levels tend to correlate with higher PM2.5 concentrations. For example, Kolkata, which experiences the highest humidity at 91%, shows the highest PM2.5 levels.
- **City-wise PM2.5 Distribution:** Manebhanjan: With a humidity level of 47%, this city shows the lowest average PM2.5 levels, indicating a possible inverse relationship between PM2.5 concentration and humidity levels at lower thresholds. Darjeeling: At 52% humidity, Darjeeling's PM2.5 levels are higher than Manebhanjan but lower than the other cities, demonstrating a moderate increase. Puri: Exhibits PM2.5 levels at 77% humidity, indicating a significant rise in pollution levels compared to Darjeeling. Purulia: With 88% humidity, Purulia shows a further increase in PM2.5 concentration, reflecting the escalating impact of humidity. Kolkata: Records the highest PM2.5 levels with 91% humidity, underlining the strong correlation between high humidity and elevated pollution levels.
- **Trend Analysis:** The graph shows a clear positive trend where cities with higher humidity percentages tend to have higher PM2.5 levels. This trend suggests that moisture in the air might contribute to the persistence and concentration of particulate matter or that areas with high humidity also suffer from other factors that elevate PM2.5 levels.

Figure 6(b) explores how PM2.5 levels fluctuate with varying air volumes measured in milliliters. The air volumes assessed are 240ml, 180ml, 120ml, and 60ml. The key Observations:

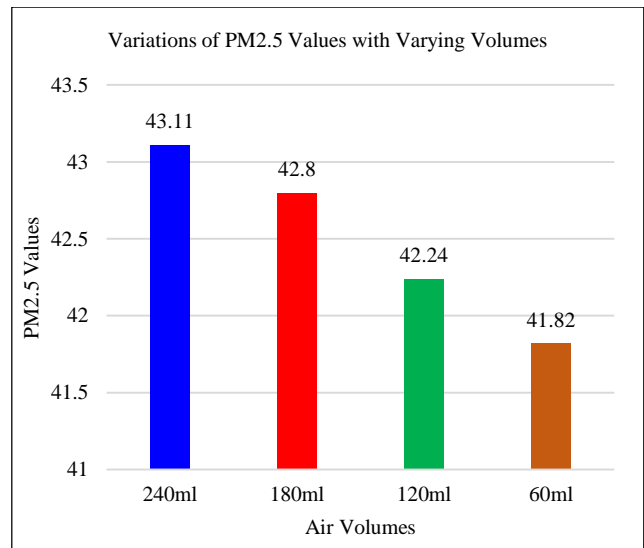
- **PM2.5 Concentration and Air Volume:** The data demonstrates an inverse relationship between air volume and PM2.5 concentrations. As the air volume decreases, the concentration of PM2.5 also tends to decrease.
- **Air Volume Analysis:** 240ml: At the highest air volume, PM2.5 values peak at 43.11. This suggests that larger air volumes may carry more particulate matter, leading to higher PM2.5 measurements. 180ml: Shows a slight decrease in PM2.5 levels (42.80), though the change is not substantial, indicating that the reduction in air volume does not linearly translate to significant changes in PM2.5 values. 120ml: A further decrease in air volume results in a noticeable drop in PM2.5 concentrations to 42.24, supporting the observation that smaller air volumes have

lower PM2.5 values.60ml: The lowest air volume yields the lowest PM2.5 concentrations at 41.82, confirming the inverse relationship between air volume and PM2.5 levels.

- **Implications:** The findings suggest that larger air volumes can collect more particulate matter, leading to higher recorded PM2.5 values. This is an important consideration for air quality monitoring, as the volume of air sampled can significantly affect the measurement of pollutant levels. These results highlight the need for standardized air volume measurements when comparing PM2.5 levels across different studies or locations.



(a)



(b)

Fig. 6 (a) Yearly average of PM2.5 levels in different cities based on varying humidity levels, and (b) Variation of PM2.5 values with varying air volumes.

The analyses of Figures 6(a) and 6(b) underscore the complexity of factors influencing PM2.5 levels in the atmosphere. Humidity and air volume are critical determinants of particulate matter concentration, with higher humidity and larger air volumes leading to increased PM2.5 levels. These findings emphasize the importance of considering environmental conditions and methodological consistency in air quality assessments. Table 3 presents the PM2.5 concentration levels ( $\mu\text{g}/\text{m}^3$ ) along with the corresponding percentage error for four cities in West Bengal: Kolkata, Kharagpur, Bankura, and Darjeeling, during three distinct seasons: summer, monsoon, and winter.

**Table 3. Comparison of the data from different environments (different places with different seasons)**

Location	Season	Adjusted PM2.5 Value ( $\mu\text{g}/\text{m}^3$ )	Yearly Average Actual ( $\mu\text{g}/\text{m}^3$ )	Percent age Error (%)
Kolkata	Summer	95	85	11.76
	Monsoon	60	70	14.29
	Winter	85	90	5.56
Average		74.33	81.67	5.56
Kharagpur	Summer	65	55	18.18
	Monsoon	40	45	11.11
	Winter	55	60	8.33
Average		46.53	53.33	10.85
Bankura	Summer	30	28	7.14
	Monsoon	15	22	31.82
	Winter	25	26	3.85
Average		23.33	25.33	7.92
Darjeeling	Summer	15	12	20.00
	Monsoon	10	13	23.08
	Winter	20	15	33.33
Average		12.75	13.33	4.35

Kolkata: Being a major urban center with heavy traffic and industrial activities, PM2.5 concentrations in Kolkata are often high throughout the year, especially in winter when atmospheric inversions trap pollutants. The annual average for Kolkata typically ranges between 60 to 100  $\mu\text{g}/\text{m}^3$  in many studies.

Kharagpur: A moderately industrial town, but with more greenery and less heavy traffic than Kolkata, Kharagpur would have a moderate PM2.5 average, likely around 40 to 60

$\mu\text{g}/\text{m}^3$ , depending on seasonal changes and industrial activities.

Bankura: A relatively rural area with lower industrial activity, so the PM2.5 concentrations should be much lower.

Darjeeling: A high-altitude region with minimal pollution sources, especially in comparison to cities, but still impacted by regional air quality. The average here is likely low, around 10 to 15  $\mu\text{g}/\text{m}^3$ .

Table 4 presents a comparative analysis of essential aspects, including reported accuracy, precision, environmental adaptability, calibration methods, and notes/findings, in a tabular format for various particulate matter sensor monitoring systems [38-42] (shown below). The evaluation focuses on the techniques used to assess particulate matter. The proposed system is presented as a more advantageous option compared to the others evaluated.

#### Comparative Insights

1. Accuracy: The accuracy of the proposed system ( $\pm 5-10\%$ ) meets or exceeds the performance of other low-cost sensors under real-world conditions.
2. Environmental Robustness: External systems like HybridLSTM show a level of adaptability. In contrast, the performance evaluation of the system across varying climates in West Bengal, including high humidity conditions in Kolkata and the dry air found in Darjeeling, suggests a degree of contextual reliability.
3. Cost-Effectiveness: The system utilizes low-cost components along with efficient calibration techniques to achieve a balance between performance and affordability. This creates a potential advantage over more advanced models, such as HybridLSTM.

## 6. Conclusion

This study investigated the influence of environmental factors-temperature, humidity, and air volume - on PM2.5 concentrations across different cities in West Bengal. The analysis revealed that PM2.5 levels are significantly higher in urban areas, such as Kolkata and Kharagpur, compared to rural or highland regions like Darjeeling. Temperature was found to affect particulate matter dispersion, with lower temperatures maintaining higher PM2.5 concentrations. Additionally, higher humidity levels were associated with increased PM2.5 concentrations, suggesting a strong relationship between moisture and particulate matter retention in the air. Lastly, varying air volumes slightly influenced PM2.5 measurements, with larger volumes capturing more particulate matter.

Overall, the study highlights the complex interplay between environmental conditions and urbanization in shaping air quality. These findings underscore the importance

of developing targeted air quality management strategies that consider local climatic conditions and urban characteristics to effectively mitigate pollution and protect public health in West Bengal.

The novelty of the proposed monitoring system lies in several key aspects that differentiate it from existing research in the field of Particulate Matter (PM<sub>2.5</sub>) monitoring systems:

1. **Low-Cost Sensor System:** The approach in this research study leverages low-cost sensors combined with robust calibration techniques, making them more accessible for real-world applications. While accurate, many existing systems are costly and require high-maintenance equipment. The affordability of this proposed system and ease of deployment are significant improvements over expensive reference-grade instruments like Tapered Element Oscillating Microbalances (TEOM) or Beta Attenuation Monitors (BAM), which are often not portable and difficult to scale for large deployments.
2. **Multi-Environmental Testing:** The research study encompassed thorough evaluations of the sensor system conducted in a variety of settings, each characterized by distinct environmental challenges. This included bustling urban centers with their complex pollution sources, heavy industrial zones marked by emissions from various manufacturing processes, and high-altitude regions such as the scenic locales of Kolkata, Kharagpur, Bankura, and Darjeeling. Through the implementation of this multi-location approach, the research intended to thoroughly evaluate the system's reliability and accuracy in the

context of diverse pollutant sources and fluctuating environmental conditions, thereby providing in-depth insights into its performance across various settings.

3. **Seasonal Adaptability:** By incorporating seasonal variations (summer, monsoon, and winter) in the calibration process, the proposed system can adapt to changing environmental factors like humidity, temperature, and air volume. This adaptability is a key strength, as many current systems do not adjust dynamically to such fluctuations.
4. **Real-Time Calibration and Processing:** The use of sophisticated calibration techniques (such as machine learning-based methods) for real-time data processing and error correction improves the accuracy of low-cost sensors, addressing a significant challenge in many existing sensor systems
5. **Practical Implementation in Public Health:** The system's potential to contribute to public health monitoring by providing a low-cost, high-accuracy solution for PM<sub>2.5</sub> monitoring in real-time makes it a valuable tool for governmental and health organizations looking to implement large-scale air quality monitoring systems without incurring high costs

The features of this research work contribute to the field by providing an effective solution for air quality monitoring, particularly in resource-constrained environments. Governments and regulatory authorities can utilize the information from this PM<sub>2.5</sub> sensor system to enhance the enforcement of air quality standards, potentially resulting in more stringent emissions regulations.

## References

- [1] Juliana P. Sá et al., "Application of the Low-Cost Sensing Technology for Indoor Air Quality Monitoring: A Review," *Environmental Technology & Innovation*, vol. 28, 2022. [[CrossRef](#)] [[Google Scholar](#)] [[Publisher Link](#)]
- [2] Jagriti Saini, Maitreyee Dutta, and Gonçalo Marques, "A Comprehensive Review on Indoor Air Quality Monitoring Systems for Enhanced Public Health," *Sustainable Environment Research*, vol. 30, 2020. [[CrossRef](#)] [[Google Scholar](#)] [[Publisher Link](#)]
- [3] Mohammad H. Forouzanfar et al., "Global, Regional, and National Comparative Risk Assessment of 79 Behavioural, Environmental and Occupational, and Metabolic Risks or Clusters of Risks in 188 Countries, 1990-2013: A Systematic Analysis for the Global Burden of Disease Study 2013," *The Lancet*, vol. 386, no. 10010, pp. 2287-2323, 2015. [[CrossRef](#)] [[Google Scholar](#)] [[Publisher Link](#)]
- [4] World Health Organization, Burden of Disease from Household Air Pollution for 2012, 2014. [Online]. Available: <https://www.ccacoalition.org/resources/world-health-organization-burden-disease-joint-effects-household-and-ambient-air>
- [5] Institute for Health Metrics and Evaluation, Global Burden of Disease (GBDx Results Tool). [Online]. Available: <http://ghdx.healthdata.org/gbd-results-tool>
- [6] Hannah Ritchie, and Max Roser, "Indoor Air Pollution," *Our World in Data*, 2014. [[Publisher Link](#)]
- [7] Stephen S. Lim et al., "A Comparative Risk Assessment of Burden of Disease and Injury Attributable to 67 Risk Factors and Risk Factor Clusters in 21 Regions, 1990-2010: A Systematic Analysis for the Global Burden of Disease Study 2010," *The Lancet*, vol. 380, no. 9859, pp. 2224-2260, 2012. [[CrossRef](#)] [[Google Scholar](#)] [[Publisher Link](#)]
- [8] Barbara A. Maher et al., "Magnetite Pollution Nanoparticles in the Human Brain," *Proceedings of the National Academy of Sciences*, vol. 113, no. 39, pp. 10797-10801, 2016. [[CrossRef](#)] [[Google Scholar](#)] [[Publisher Link](#)]
- [9] World Health Organization, Public Health, Environmental and Social Determinants of Health (PHE) during the Seventieth World Health Assembly, Geneva, Switzerland, 2017. [Online]. Available: [https://www.who.int/news-room/events/detail/2017/05/22/default-calendar/public-health-environmental-and-social-determinants-of-health-\(phe\)-during-the-70th-world-health-assembly](https://www.who.int/news-room/events/detail/2017/05/22/default-calendar/public-health-environmental-and-social-determinants-of-health-(phe)-during-the-70th-world-health-assembly)
- [10] Hyuntae Cho, "Personal Environmental Monitoring System and Network Platform," *2015 9th International Conference on Sensing Technology (ICST)*, Auckland, New Zealand, pp. 751-756, 2015. [[CrossRef](#)] [[Google Scholar](#)] [[Publisher Link](#)]

- [11] Jonathan O. Anderson, Josef G. Thundiyil, and Andrew Stolbach, "Clearing the Air: A Review of the Effects of Particulate Matter Air Pollution on Human Health," *Journal of Medical Toxicology*, vol. 8, pp. 166-175, 2012. [[CrossRef](#)] [[Google Scholar](#)] [[Publisher Link](#)]
- [12] George F. Fine et al., "Metal Oxide Semi-Conductor Gas Sensors in Environmental Monitoring," *Sensors*, vol. 10, no. 6, pp. 5469-5502, 2010. [[CrossRef](#)] [[Google Scholar](#)] [[Publisher Link](#)]
- [13] Brigida Alfano et al., "A Review of Low-Cost Particulate Matter Sensors from the Developers' Perspectives," *Sensors*, vol. 20, no. 23, 2020. [[CrossRef](#)] [[Google Scholar](#)] [[Publisher Link](#)]
- [14] Amara L. Holder et al., "Field Evaluation of Low-Cost Particulate Matter Sensors for Measuring Wildfire Smoke," *Sensors*, vol. 20, no. 17, 2020. [[CrossRef](#)] [[Google Scholar](#)] [[Publisher Link](#)]
- [15] Hoochang Lee et al., "Long-Term Evaluation and Calibration of Low-Cost Particulate Matter (PM) Sensor," *Sensors*, vol. 20, no. 13, 2020. [[CrossRef](#)] [[Google Scholar](#)] [[Publisher Link](#)]
- [16] Erika Brattich et al., "How to Get the Best from Low-Cost Particulate Matter Sensors: Guidelines and Practical Recommendations," *Sensors*, vol. 20, no. 11, 2020. [[CrossRef](#)] [[Google Scholar](#)] [[Publisher Link](#)]
- [17] Steven J. Johnston et al., "City Scale Particulate Matter Monitoring Using LoRaWAN Based Air Quality IoT Devices," *Sensors*, vol. 19, no. 1, 2019. [[CrossRef](#)] [[Google Scholar](#)] [[Publisher Link](#)]
- [18] Sara Zanni et al., "Indoor Air Quality Real-Time Monitoring in Airport Terminal Areas: An Opportunity for Sustainable Management of Micro-Climatic Parameters," *Sensors*, vol. 18, no. 11, 2018. [[CrossRef](#)] [[Google Scholar](#)] [[Publisher Link](#)]
- [19] Andrea Di Antonio et al., "Developing a Relative Humidity Correction for Low-Cost Sensors Measuring Ambient Particulate Matter," *Sensors*, vol. 18, no. 9, 2018. [[CrossRef](#)] [[Google Scholar](#)] [[Publisher Link](#)]
- [20] Stephen Reece et al., "Spatial-Temporal Analysis of PM<sub>2.5</sub> and NO<sub>2</sub> Concentrations Collected Using Low-Cost Sensors in Peñuelas, Puerto Rico," *Sensors*, vol. 18, no. 12, 2018. [[CrossRef](#)] [[Google Scholar](#)] [[Publisher Link](#)]
- [21] Shaohua Hu et al., "Evaluation of Gravimetric Method to Measure Light-Duty Vehicle Particulate Matter Emissions at Levels below One Milligram per Mile (1 mg/mile)," SAE Technical Paper 2014-01-1571, 2014. [[CrossRef](#)] [[Google Scholar](#)] [[Publisher Link](#)]
- [22] So Eun Shin, Chang Hoon Jung, and Yong Pyo Kim, "Analysis of the Measurement Difference for the PM<sub>10</sub> Concentrations between Beta-Ray Absorption and Gravimetric Methods at Gosan," *Aerosol and Air Quality Research*, vol. 11, pp. 846-853, 2011. [[CrossRef](#)] [[Google Scholar](#)] [[Publisher Link](#)]
- [23] Harvey Patashnick, and Erich G. Rupperecht, "Continuous PM-10 Measurements Using the Tapered Element Oscillating Microbalance," *Journal of the Air & Waste Management Association*, vol. 41, no. 8, pp. 1079-1083, 1991. [[CrossRef](#)] [[Google Scholar](#)] [[Publisher Link](#)]
- [24] World Health Organization, *WHO Guidelines for Indoor Air Quality: Selected Pollutants*, WHO, Geneva, Switzerland, 2010. [[Google Scholar](#)] [[Publisher Link](#)]
- [25] Karoline K. Johnson et al., "Using Low Cost Sensors to Measure Ambient Particulate Matter Concentrations and On-Road Emissions Factors," *Atmospheric Measurement Techniques Discussions*, 2016. [[CrossRef](#)] [[Google Scholar](#)] [[Publisher Link](#)]
- [26] Sinan Sousan, Swastika Regmi, and Yoo Min Park, "Laboratory Evaluation of Low-Cost Optical Particle Counters for Environmental and Occupational Exposures," *Sensors*, vol. 21, no. 12, 2021. [[CrossRef](#)] [[Google Scholar](#)] [[Publisher Link](#)]
- [27] Janani Venkatraman Jagatha et al., "Calibration Method for Particulate Matter Low-Cost Sensors Used in Ambient Air Quality Monitoring and Research," *Sensors*, vol. 21, no. 12, 2021. [[CrossRef](#)] [[Google Scholar](#)] [[Publisher Link](#)]
- [28] Martha Arbayani Zaidan et al., "Intelligent Calibration and Virtual Sensing for Integrated Low-Cost Air Quality Sensors," *IEEE Sensors Journal*, vol. 20, no. 22, pp. 13638-13652, 2020. [[CrossRef](#)] [[Google Scholar](#)] [[Publisher Link](#)]
- [29] S.K. Sharma, and T.K. Mandal, "Elemental Composition and Sources of Fine Particulate Matter (PM<sub>2.5</sub>) in Delhi, India," *Bulletin of Environmental Contamination and Toxicology*, vol. 110, 2023. [[CrossRef](#)] [[Google Scholar](#)] [[Publisher Link](#)]
- [30] Georgia Miskell, Jennifer A. Salmond, and David E. Williams, "Solution to the Problem of Calibration of Low-Cost Air Quality Measurement Sensors in Networks," *ACS Sensors*, vol. 3, no. 4, pp. 832-843, 2018. [[CrossRef](#)] [[Google Scholar](#)] [[Publisher Link](#)]
- [31] Mariusz Rogulski, and Artur Badyda, "Investigation of Low-Cost and Optical Particulate Matter Sensors for Ambient Monitoring," *Atmosphere*, vol. 11, no. 10, 2020. [[CrossRef](#)] [[Google Scholar](#)] [[Publisher Link](#)]
- [32] Hyuntae Cho, and Yunju Baek, "Practical Particulate Matter Sensing and Accurate Calibration System Using Low-Cost Commercial Sensors," *Sensors*, vol. 21, no. 18, 2021. [[CrossRef](#)] [[Google Scholar](#)] [[Publisher Link](#)]
- [33] Naser Hossein Motlagh et al., "Transit Pollution Exposure Monitoring Using Low-Cost Wearable Sensors," *Transportation Research Part D: Transport and Environment*, vol. 98, 2021. [[CrossRef](#)] [[Google Scholar](#)] [[Publisher Link](#)]
- [34] Alicia Gressent et al., "Data Fusion for Air Quality Mapping Using Low-Cost Sensor Observations: Feasibility and Added-Value," *Environment International*, vol. 143, 2020. [[CrossRef](#)] [[Google Scholar](#)] [[Publisher Link](#)]
- [35] Andrea L. Clements et al., "Low-Cost Air Quality Monitoring Tools: From Research to Practice (A Workshop Summary)," *Sensors*, vol. 17, no. 11, 2017. [[CrossRef](#)] [[Google Scholar](#)] [[Publisher Link](#)]
- [36] Jianzhao Bi et al., "Incorporating Low-Cost Sensor Measurements into High-Resolution PM<sub>2.5</sub> Modeling at a Large Spatial Scale," *Environmental Science & Technology*, vol. 54, no. 4, pp. 2152-2162, 2020. [[CrossRef](#)] [[Google Scholar](#)] [[Publisher Link](#)]

[37] Esmeralda Mendez et al., “Using Low-Cost Sensors to Assess PM<sub>2.5</sub> Concentrations at Four South Texan Cities on the U.S.-Mexico Border,” *Atmosphere*, vol. 13, no. 10, 2022. [[CrossRef](#)] [[Google Scholar](#)] [[Publisher Link](#)]

[38] Jianwei Huang et al., “Field Evaluation and Calibration of Low-Cost Air Pollution Sensors for Environmental Exposure Research,” *Sensors*, vol. 22, no. 6, 2022. [[CrossRef](#)] [[Google Scholar](#)] [[Publisher Link](#)]

[39] Jiayu Li et al., “Evaluation of Nine Low-Cost-Sensor-Based Particulate Matter Monitors,” *Aerosol and Air Quality Research*, vol. 20, no. 2, pp. 254-270, 2020. [[CrossRef](#)] [[Google Scholar](#)] [[Publisher Link](#)]

[40] Donggeun Park et al., “Assessment and Calibration of a Low-Cost PM<sub>2.5</sub> Sensor Using Machine Learning (Hybrid LSTM Neural Network): Feasibility Study to Build an Air Quality Monitoring System,” *Atmosphere*, vol. 12, no. 10, 2021. [[CrossRef](#)] [[Google Scholar](#)] [[Publisher Link](#)]

[41] Kamaljeet Kaur, and Kerry E. Kelly, “Performance Evaluation of the Alphasense OPC-N3 and Plantower PMS5003 Sensor in Measuring Dust Events in the Salt Lake Valley, Utah,” *Atmospheric Measurement Techniques*, vol. 16, no. 10, pp. 2455-2470, 2023. [[CrossRef](#)] [[Google Scholar](#)] [[Publisher Link](#)]

[42] Minxing Si et al., “Evaluation and Calibration of a Low-Cost Particle Sensor in Ambient Conditions Using Machine-Learning Methods,” *Atmospheric Measurement Techniques*, vol. 13, no. 4, pp. 1693-1707, 2020. [[CrossRef](#)] [[Google Scholar](#)] [[Publisher Link](#)]

**Appendix**

**Table 4. A comparative analysis with existing air quality monitoring systems**

Sensor/System	Reported Accuracy/Precision	Environmental Adaptability	Calibration Method	Notes/Findings
Proposed System in this research study	±5–10% error; strong calibration model	Handles varying humidity, temperature, and air volumes	Polynomial regression and Kalman filter	Demonstrated reliability across diverse West Bengal regions; cost-effective with robust performance under various conditions.
AirBeam2 [38]	±15–20% error in urban environments	Declines in high humidity; performs well in urban dry areas	Random Forest machine learning	Moderate accuracy under varied conditions; strong correlation (R <sup>2</sup> ~ 0.85) with reference-grade instruments
PurpleAir PA-II-SD [39]	±10% compared to reference systems	Effective for ambient outdoor air monitoring	Factory-calibrated	High reliability in standard conditions; limited by extreme humidity or temperature variations
HybridLSTM Model [40]	RMSE reduced by 41–60%	Adapts dynamically to industrial and urban conditions	Neural network (HybridLSTM)	Achieved R <sup>2</sup> of 93%, outperforming traditional linear models and uncalibrated sensor outputs
Alphasense OPC-N3 [41]	±5–10% for PM <sub>2.5</sub> and PM <sub>10</sub>	Robust across wide airflow and particle size distributions	Polynomial regression	Effective in detecting a broad range of particle sizes in both indoor and outdoor conditions
Plantower PMS 1003 [42]	Deviations up to 46% in foggy conditions	Affected by high humidity/fog; high linearity otherwise	Light-scattering model adjustments	Overestimates concentrations under extreme environmental conditions; high linearity (R <sup>2</sup> > 0.89)